Prediction of Acoustic Velocity Properties of Downed Pine Trees Using Near-Infrared Spectroscopy

Munkaila Musah Abiodun O. Alawode Javier Hernandez Diaz
Osei Asafu-Adjaye Tom Gallagher Maria S. Peresin
Yucheng Peng Dana Mitchell Mathew Smidt Brian Via

Abstract

Near-infrared reflectance (NIR) spectroscopy was used to determine correlations between acoustic velocity and stiffness properties of downed pine trees in the southern coastal plains of the United States. Three acoustic measurement methods (longitudinal, transverse, and offset) were used. From the measurement of the acoustics, the time of flight (TOF) was determined from the downed trees. Increment core samples were obtained from each thirty downed pine trees in the study. NIR spectra were obtained using a fiber probe on the radial surface of each core to rapidly correlate the speed of sound, estimate the strength properties of the downed trees, and the TOF acoustic assessments. The NIR prediction was very good for the transverse and offset methods. The predictability diagnostic was above an R^2 of 0.70 for both offset measurements for the transverse methods for the acoustic velocity and dynamic modulus of elasticity (MOE). The longitudinal measurement exhibited the weakest model ($R^2 < 0.65$) for both the acoustic velocity and the MOE with the highest standard error of prediction between 3.0 (EL_{VLSWV}) and 0.31 (V_{LSWV}) for the three measurement types. All the standard errors of calibration were below 1% except in EL_{VOSWV}, which was ~2%. The dry density measured from the increment cores had a moderate correlation ($R^2 \sim 60\%$), compared with the lower correlation ($R^2 \sim 50\%$) by the green density in the multiple linear regression output. The results of the acoustic model indicated that NIR spectroscopy has the potential to predict the acoustic velocity and corresponding stiffness of downed trees.

Weather events such as hurricanes and tornadoes cause significant damage to trees, which require a good assessment of their physical and mechanical properties to help extract the best value products. The modulus of elasticity (MOE) is a measure of stiffness and is often used as a surrogate to classify lumber and, more recently, logs. MOE cannot be determined visually for trees; therefore, both destructive and nondestructive approaches have been adopted in tree assessments. However, destructive procedures require extensive and costly sample preparation and testing. Considering the large number of trees that must be assessed during hurricane and tornado events, conventional destructive methods will not be practical and feasible. The industry would thus benefit from rapid, nondestructive, and cost-effective alternatives such as acoustic technologies and near-infrared spectroscopy (NIR) estimations.

To develop accurate models for the prediction of wood mechanical properties, repurposing, and use of downed timber along the supply chain, more rapid and accurate methods of compositional analysis are needed. NIR coupled with multivariate data analysis is proven to be a fast and nondestructive analytical tool in the prediction of internal wood quality traits, including storm-damaged trees (Downes et al. 2000, 2014; Gindl et al. 2001; Thumm and Meder 2001; Via et al. 2003; Kelley et al. 2004; Tsuchikawa 2007;

The authors are, respectively, Assistant Professor, Dept. of Environ. Conservation, Univ. Massachusetts, Amherst; Research Scientist, Research Assistant, and Research Scientist, School of Forestry and Wildlife Sci., Auburn Univ., Auburn, Alabama, and Forest Products Development Center, Auburn Univ., Auburn, Alabama; Professor, School of Forestry and Wildlife Sci., Auburn Univ., Auburn, Alabama; Professor and Professor, School of Forestry and Wildlife Sci., Auburn Univ., Auburn, Alabama, and Forest Products Development Center, Auburn Univ., Auburn, Alabama; Technology Manager, U.S. Dept. of Energy, Bioenergy Technol. Office, Washington, DC; Research Forester, USDA Forest Serv., Southern Research Sta., Auburn, Alabama; and Professor, School of Forestry and Wildlife Sci., Auburn Univ., Auburn, Alabama, and Forest Products Development Center, Auburn Univ., Auburn, Alabama. This paper was received for publication in November 2022. Article no. 22-00067.

Forest Prod. J. 73(2):133–141.
doi:10.13073/FPJ-D-22-00067

Wang et al. 2010; Cieszewski et al. 2013; Zhao et al. 2013; Tsuchikawa and Kobori 2015).

Reliable and rapid techniques for nondestructive assessment of wood and other forest products can improve financial return and reduce wood waste. Studies by Legg and Bradley (2016) also concluded that having a good understanding of tree stiffness could be used to improve breeding, planting, and silviculture management for better future forests. Field and laboratory-based tools such as NIR (Horvath et al. 2011, Viet et al. 2021), acoustics (Wang et al. 2001, Wang et al. 2007a, Wang et al. 2007b), pilodyn (Cown 1978, Raymond and MacDonald 1998, Wu et al. 2010, Wessels et al. 2011, Chen et al. 2015, Gao et al. 2017), resistograph (Downes et al. 2018, Gendvilas et al. 2021), rigidimeter (Launay et al. 2000, 2002), computed tomography (CT) scanning (Hou et al. 2009, Beaulieu and Dutilleul 2019), the Scion's DiscBot (Schimleck et al. 2019), and SilviScan (Mora et al. 2009), among others, can be used to assess the density and strength properties of standing trees, logs, damaged trees, and samples obtained from an increment core, stem, or disc of the tree. In addition to the NIR, sound wave propagation (acoustic technologies) has also proven a useful and reliable rapid tool for the assessment of tree inner qualities (Wang et al. 2001, Pellerin and Ross 2002, Dickson et al. 2004, Legg and Bradley 2016).

Studies by Schimleck et al. (2001) estimated several physical and mechanical properties of different pine species using NIR spectroscopy where the density ($R^2 = 0.81$, standard error of cross-validation, $\text{SECV} = 38.5\ \text{kg/m}^3$) and MOE ($R^2 = 0.81$, $\text{SECV} = 1124$ GPa) diagnostics demonstrated that it was possible to obtain general calibrations for estimation of wood properties in several tropical, subtropical, and temperate pine species. Kohan et al. (2013) modeled the ultimate tensile strength, tensile MOE, bending strength, and bending stiffness of strand feedstock mechanical properties and found that the MOE for strands under bending exhibited the strongest correlation ($R^2 = 0.76$). NIR has also been used to estimate density (Alves et al. 2012), and monitor wood heat treatment (Mitsui et al. 2008), and NIR has been applied in many different sectors, including agriculture (Batten 1998, Mitsui et al. 2008, Dale et al. 2013, Vincent and Dardenne 2021), pharmaceuticals (Luypaert et al. 2007, Palou et al. 2012), food industry (Prevolnik et al. 2004), and other fields (Hoffmeyer and Pedersen 1995, Fomina et al. 2011, Maji et al. 2019).

Spectroscopy investigates the interaction between matter and the photons of electromagnetic radiation (EMR) in the form of electric and magnetic waves. The NIR region covers the range from 4,000 to 14,000 cm^{-1} (2.5 to 0.7 mm), allowing the absorption of electromagnetic wavelength by organic molecules in this spectral range due to vibrations and excitations of overtones and combinations of fundamental elements of C–H, O–H, and N–H (Hoffmeyer and Pedersen 1995, Gäb et al. 2006, Schimleck et al. 2018).

Despite the advancement in the use of NIR in assessing tree properties, which has proven effective for assessing and monitoring biomaterial quality, there is quite a knowledge gap when used with acoustics. While the studies by Nasir et al. (2019) used longitudinal stress waves generated by a pendulum impact from a Metriguard 239A for velocity assessment and estimated dynamic MOE (MOEdy) using the Adaptive neuro-fuzzy inference system (ANFIS), our current approach focused on using the NIR principal component regression (PCR) + quantitative to predict acoustic velocity using the different probe positioning strategies. Hence, this current study focuses on using different probe positioning strategies and NIR as rapid approaches in assessing tree stiffness, which is one of the hindrances of the use of storm-damaged downed timber. Understanding the stiffness will help landowners classify downed timber into product classes that might not have been considered by the landowner previously. Hence, this study used and compared three different acoustic velocity sampling methods and the ability to use NIR spectroscopy as a surrogate prediction tool.

Methodology

Near-infrared spectroscopy

The infrared (IR) region lies between the visible and microwave regions of the electromagnetic spectrum. NIR measures the amount of near-infrared light a sample absorbs, transmits, or reflects based on its chemical composition. A Perkin Elmer Spectrum 400 Fourier-transform infrared (FT-IR)/FT-NIR spectroscope was used to collect the NIR spectra from the radial face of the dried core samples, with the smoothest surface used for spectra collection. To meet the statistical requirements, replicate scans were taken on each of the core samples from the 30 different trees. The 1,860 scans acquired were averaged to 30 spectra, with each spectrum obtained by averaging 62 independent scans. All 30 spectra from the averaged scans were used for prediction, and 15 samples from the crown region were used for calibration. Since the thickness of the samples was 1.0 ± 0.03 mm, it was assumed that the wood chemistry on both faces was equal. Absorbance was recorded from 1,000 to 25,000 nm with a resolution of 0.5 nm with 64 scans. All NIR measurements were made in a controlled environment of 40 percent relative humidity and a temperature of 20°C.

Core samples from downed trees

Thirty downed trees were selected from two different diameter classes at breast height (Chip-N-Saw 8 to 10.9 in. and saw logs 11 in. up) for the development of acoustic velocity measurement. Fresh core samples were taken from each downed tree. The samples were dried in a vacuum freeze drier (The Labconco 6 Liter Console Freeze Dry System with 16-port round drying and Edwards RV8 Vacuum Pump, Hampton, New Hampshire) operating at a condenser temperature of –50°C and a vacuum pressure of 10 Pa 48 hours (Hammami et al. 1999). The moisture-free core samples were cut to a thickness of 1.0 mm and taken to the Perkin Elmer Spectrum 400 FT-IR/FT-NIR spectroscope for analysis.

Downed tree properties and sound waves

The Fakopp 1D Microsecond Timer (Fakopp Enterprise, Agfalva, Hungary) was used to measure stress wave velocity that was transmitted and received via two probes inserted into the sapwood of each tree at a 45-degree angle pointed toward each other as shown in Figure 1 (Wang et al. 2007b). The transverse (V_{TSWV}), longitudinal (V_{LSWV}), and the opposite phase (offset) (V_{OSWV}) methods used in this study are shown in Figure 1 as described in Musah et al. (2022).

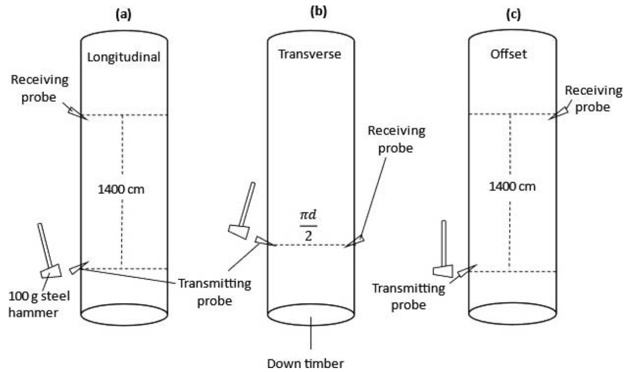

Figure 1.—The three different patterns of acoustic measurement (a) longitudinal, (b) transverse, and (c) offset method.

The green and dry densities were estimated from the increment core samples of the downed trees (Ross 2010). The stiffness is related to the dynamic modulus of elasticity (MOEdy); E_L was estimated by measuring the velocity of the traveling wave and by using the one-dimensional wave equation (Wang et al. 2002, Wang 2013) indicated in Equations 1 and 2.

$$V = \sqrt{\frac{\text{MOEdy}}{\rho}} \tag{1}$$

$$\text{MOEdy} = \text{EL} = V2 \times \rho \tag{2}$$

where MOEdy or EL (Gpa) is the dynamic modulus of elasticity, V (km/s) is the one-dimensional wave velocity, and r (kg/m^3) is the bulk density of the wood (estimated from the oven dry methods).

Multivariate analysis

Multivariate calibration is one of the major success stories of chemometrics, owing to a large number of applications in NIR spectroscopy (Martens and Martens 2001). The chemometric approach to quantification provides a choice of multivariate calibration algorithms. This algorithm gives reliable model output obtained using multivariate calibration methods such as partial least squares (PLS) regression and principal component regression (PCR). This study used both PCR and PLS regression to calibrate the NIR spectra and compare the three different methods of acoustic estimation and their corresponding NIR prediction. Studies have indicated that PCR could yield simple and better models for cases where the interpretation of the model was important (Jouan-Rimbaud et al. 1995, Via et al. 2014). PLS is mostly shown to perform better than PCR when dealing with low-detection limit samples (Lipp 1996).

Calibration development and statistics

To analyze the NIR results, PLS regression models with four cross-validation segments were used for calibration development and optimization. The PerkinElmer Spectrum Quant+ software was used for all the analyses with a spectral signature measured between 10,000 and 4,000 cm^{-1}. Cores from all 30 downed timber trees were used for the calibration. Second-derivative spectra with a segment of 10 nm were used to develop the NIR analysis systems. Regression diagnostics were used to compare the predictive power of different models. Each tree model was deduced from the 20 scans taken from the core samples. In total, 15 core samples from the crown region of 15 trees from the site were used for building the validation model. Regression coefficients, root mean square error of validation (RMSEV), R^2, and the adjusted R^2 were used to compare the model predictability. The equation for the RMSEV used was

$$\text{RMSEV} = \sqrt{\frac{\sum_{i-1}^{i=n} (y_i - \hat{y}_i)^2}{n}}$$

where y_i is the prediction value of the ith observation, $\hat{y}_i$ is the measured value of the observation, and n is the number of observations. The RMSEV for this paper was the root mean square error derived when regressing the calibration model to the validation data. A lower RMSEV and a higher R^2 and adjusted R^2 suggest a better model. The NIR-based models were developed by correlating the spectra data with basic density, acoustic velocity, and MOEdy by the partial least squares regression. The matrix was composed of estimated values of the stress wave timer and physical analyses (determined by standardized procedures) and by the NIR spectra collected in the respective core samples of the trees. The mathematical models for the spectra included central averaging, normalization, first derivative, and second derivative with a 10-point filter and a second-order polynomial. The leave-one-out method was used for full cross-validations, while independent set validation was performed using spectra from the 15 trees chosen at random.

The PLS algorithm used the data decomposition technique to extract the systematic variation that exists in the data set by using the raw untreated NIR spectra (i.e., absorption of NIR light at different wavelengths) as the independent (X) variables and regressed them on the results acquired from the conventional testing methods (that is dependent – Y variables). The regression of the PLS involves simultaneous and interdependent principal components analysis (PCA) decomposition of both the X and Y matrix. The measured absorbance of NIR of the cores of the downed trees at the wavelength is related to the acoustic and strength properties or other concentrations of the analyte of interest based on the Bouguer-Lambert-Beer or, more commonly, Beer's law, indicated in Equation 3 (Burns and Ciurczak 2007). Several statistics, including standard error of calibration (SEC), standard error of prediction (SEP), coefficient of determination (R^2), and residual predictive deviation/ratio of performance to deviation (RPD), were used to evaluate the performance of our models. Models that had the least error values were selected and used to predict the acoustic velocity and MOEdy of the downed timber. The measure of how well a calibration fits the data is the SEC. The measure of how well the calibration predicts the constituent of interest for a set of unknown samples that are different from the calibration test set is given by the SEP. Formulas used to estimate the SEC and SEP given in Schimleck and Evans (2002) are indicated in Equations 4 and 5, respectively.

$$A = \log_{10} \frac{I_0}{I} \tag{3}$$

$$\text{SEC} = \sqrt{\frac{\sum_{i=1}^{\text{NC}} (\hat{y}_i - y_i)^2}{\text{NC} - k - 1}} \tag{4}$$

$$\text{SEP} = \sqrt{\frac{\sum_{i=1}^{\text{NP}} (\hat{y}_i - y_i)^2}{\text{NP} - k - 1}} \qquad (5)$$

where A is the absorbance; I_0 is the intensity of radiation entering the sample; I is the intensity of radiation transmitted by the sample; $\hat{y}_i$ is the value of the constituent of interest for the validation sample in SEC and the value of the constituent of interest for the sample in the SEP; i is estimated using the calibration in SEC and predicted by the calibration in SEP; y_i is the known value of the constituent of interest of sample i; NC is the number of samples used to develop the calibration; k is the number of factors used to develop the calibration; y_i is the known value of the constituent of interest for sample i in both SEC and SEP; NP is the number of samples in the prediction set; NC is the number of samples used to develop the calibration; and k is the number of factors used to develop the calibration.

The PCR+ algorithm

This study used the PCR+ quantitative technique to establish the relationship between the property of interest. One for each component between the spectra of a set of calibration standards, and the corresponding property values determined by independent means (density, MOEdy, and velocity). These relationships can be used for the subsequent prediction of unknown samples.

Results

NIR model calibration and evaluation

Organic compounds consist of various functional groups whose molecular vibration is observed in the IR range. The absorptivity of NIR light in organic materials is very weak compared to that of IR light, which could measure high-density and concentration materials directly using NIR light (Tsuchikawa and Kobori 2015). Chemometrics, which involves the aid of computers and mathematics, is then applied to the spectra to derive meaningful interpretations of chemical information from samples of varying complexity. The NIR spectra for downed loblolly pine trees (Fig. 2) and property calibrations developed for the downed trees are given in Table 1. To avoid overfitting, the minimum SEP was used for choosing the best number of principal components. There were positive and strong associations with the acoustic velocity (V_{TSWV}, V_{OSWV}) and modulus of elasticity (EL_{VTSWV}, EL_{VOSWV}) with coefficients of determination (R^2) above 70 percent. The longitudinal measuring method for both acoustics velocity (V_{LSWV}) and the modulus of elasticity (EL_{VLSWV}) demonstrated a moderate association ($R^2 \sim 50\%$). The R^2 for the dry density was above 60 percent, which was higher than the green density ($R^2 = 51.5\%$). The standard errors (SEC) were not far from each other and below 1.0, except in EL_{VLSWV} (SEC =2.37). However, similar SEC across categories indicates that calibrations based on the NIR spectra of downed loblolly pine core samples can be used to predict wood properties that are shown in Raymond et al. (2001) and Raymond and Schimleck (2002), where NIR spectra from milled increment cores were used to estimate properties of wood in Tasmanian bluegum (*Eucalyptus globulus* Labill.) and to assess the quality of its wood pulp.

Table 1.—Summary statistics of calibration developed for downed pine trees.

Downed tree property	No. of factors	R^2 (% variance)	SEC	SEP	MPV
EL_{VLSWV} (GPa)	6	50.09	0.25	0.306	3.50
EL_{VOSWV} (GPa)	7	70.43	2.37	3.00	5.37
EL_{VTSWV} (GPa)	7	70.61	0.78	0.89	6.59
Dry density (g/cm^3)	7	60.39	0.05	0.06	0.49
Green density (g/cm^3)	7	51.51	0.08	0.08	0.85
V_{LSWV} (km/s)	8	50.27	0.25	0.31	3.50
V_{OSWV} (km/s)	7	70.55	0.29	0.30	5.37
V_{TSWV} (km/s)	8	75.10	0.12	0.17	2.76

The data for the absorbance of downed timber spectra grouped by age and separated by their mean density are shown in Figure 3. The spectra were collected over the whole range of 4,000 cm^{-1} (2,500 nm) wave number to about 10,000 cm^{-1}. The data for the transmittance, based on the mean density of the trees, showed a clear distinction in the transmittance percentage for each age group. The denser

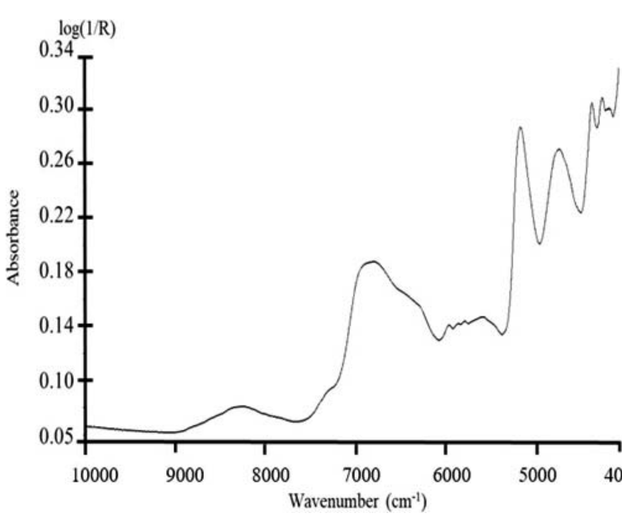

Figure 2.—Typical absorbance spectra of downed pine trees.

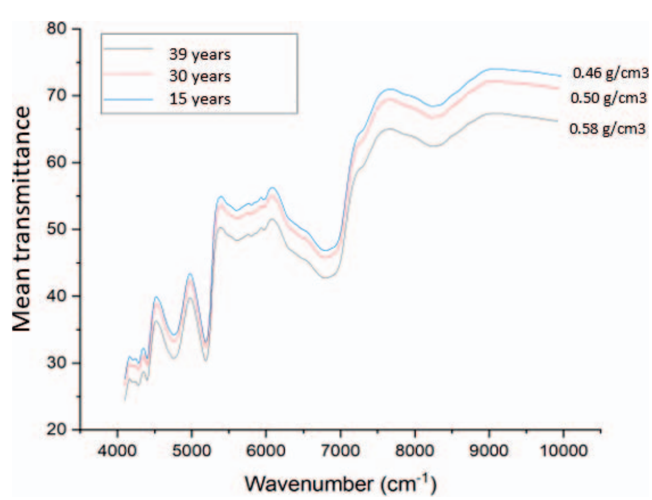

Figure 3.—The transmittance of downed pine trees, classified by age: 15-yr-old trees, 30-yr-old trees, and 39-yr-old downed pine trees.

group (39 yr) recorded a low transmittance percentage compared to the less dense age group (15 yr). The older trees absorbed more incident radiation compared to the younger trees, probably due to the increased density in the visible light section of the electromagnetic spectrum (4×10^{-7} m to 7×10^{-7} m), which resulted in low transmittance. The relatively lower transmittance at the blue-light spectral region is most likely due to absorption by the lignin. However, the wavelength dependence does not have a strong effect and does not strongly influence the total transmittance. Fujimoto et al. (2012) accurately predicted wood density using NIR spectra obtained from 100 Japanese larch (*Larix kaempferi*) wood samples containing various amounts of moisture, where characteristic absorbance bands in the vicinity of 7,320 cm^{-1} (1,366 nm), 7,160 cm^{-1} (1,400 nm), and 7,000 cm^{-1} (1,428 nm) were key in predicting wood density. The air-dried wood showed the highest absorption values at peaks 7,320 cm^{-1} and 7,000 cm^{-1}, indicating that wood density could be estimated independently of moisture content.

The transmittance data for the downed pine trees and the second-derivative spectra, which measured the rate of the absorbance change to the wavelength at the first derivative with the different age groups, are presented in Figure 4. Comparing the labeled spectra to the literature on band assignment in near-infrared spectra of wood and wood components (Schwanninger et al. 2011), the peak at 4,411 cm^{-1} (2,267 nm) can be assigned to lignin, 4,808 cm^{-1} (2,080 nm) is assigned to semicrystalline or crystalline regions in cellulose, 5,245 cm^{-1} (1,907 nm) is assigned to hemicellulose, and 6,003 cm^{-1} (1,666 nm) is assigned to hemicellulose at a bond vibration of first overtone C–H str. (CH_3 groups). The peak at 7,092 cm^{-1} is assigned to lignin/extractives that are phenolic hydroxyl groups or from lignin (Baillères et al. 2002) as reported by Wüst and Rudzik (1996).

The number of factors used in the model was comparable with those reported by Schimleck et al. (2018), who modeled the NIR spectroscopy for the estimation of density (at 12% moisture content), MOEdy, and modulus of rupture using clear wood samples obtained from several pine species with transmitted NIR spectra from increment cores.

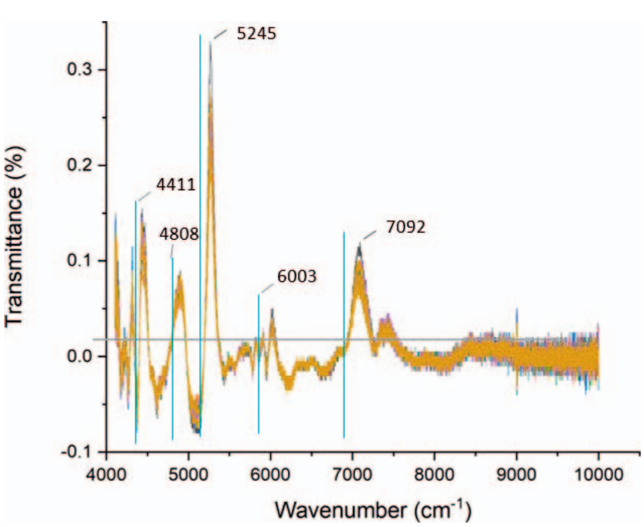

Figure 4.—Second derivative of the transmittance of the downed pine trees.

However, the required number of factors in the present study was considerably more than those reported by most of the other studies. This is probably due to the large spectral variation caused by the differences in the stand age and diameter at breast height (dbh) classes.

Estimated acoustic velocity and NIR predicted acoustic velocity

The primary objectives of this study were to access the predictive accuracies of three different types of acoustic measurement positions and corresponding predictive acoustic stiffness with NIR as a nondestructive evaluation approach. NIR has been used to model nonchemistry secondary traits such as density (Fujimoto et al. 2012), acoustic velocity, and strength properties of wood with the aid of chemometrics where cellulosic features have an underlying effect. Several studies have shown that acoustics have been used for both juvenile wood (Lindstrom et al. 2002, 2004), mature wood (Chauhan and Walker 2004, Lindstrom et al. 2005), and standing or felled logs (Legg and Bradley 2016). Even though the relationship between the reduced model ($PC \leq 7$) of the estimated acoustics velocity and the NIR predicted measurements for the three measurements ranged from 50 to 70 percent, the calculated data from the multiple linear regression for the full model ($7 \leq PC \leq 10$) of the properties ranged from about 60 to ~80 percent (Fig. 5). Caution needs to be established in the use of the full model due to overfitting. The full model indicates the association of the NIR predicted and established measured properties. The regression analysis indicated a linear correlation between the time of flight (TOF) of downed trees for each method tested and the core sample predicted by the NIR. The range of acoustic velocity values predicted for the downed loblolly pine was from 2.40 to 3.33 km/s for the transverse acoustic velocity (V_{TSW}), 5.16 to 6.05 km/s for the offset/opposite face method (V_{OSW}), and 3.24 to 4.10 km/s for the longitudinal acoustic velocity. The relationship between estimated acoustics and the NIR predicted acoustic velocity based on the coefficient of determination for the offset (V_{OSW}) and the transverse (V_{TSW}) were similar (>70%), while the longitudinal (V_{LSW}) was a little on the low side (63% at PC 8). This difference between the three different methods was attributed to the differences in the path of travel by the stress wave and the amount of wood through which the stress wave must pass

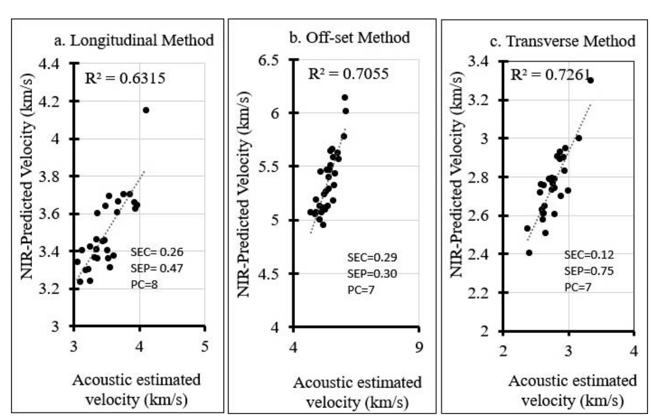

Figure 5.—Relationship between measured acoustic velocity and NIR-fitted velocity.

(Schimleck et al. 2018). The 30 downed loblolly pines used in this study ranged from 15 to 40 years of age. The NIR predicted acoustic velocity of the downed pines was comparable to several other studies' TOF acoustic measurements: An average of 1.88 to 2.88 km/s was estimated for stands with ages within 8 to 25 years for studies conducted by Chauhan and Walker (2006). The larger and older trees recorded higher acoustic velocities both in the TOF estimation and in the NIR predicted compared to younger trees.

Laboratory estimated density and NIR predicted density

The ranges of the NIR predicted green density (0.65 to 0.99 g/cm^3) and dry density (0.40 to 0.58 g/cm^3), compared to the acoustic measurements (0.69 to 0.95 g/cm^3 for green density and 0.40 to 0.59 g/cm^3 for the dry density) is shown in Figure 6. The R^2 for the dry density was higher than the green density, possibly due to the near equal moisture and weight in the cores leading to less variability in the green density as seen in both the acoustically measured and the NIR predicted outcomes for the downed trees in this study. The NIR results output for this study is similar to the ranges of results obtained by (Belonger et al. 1997) (0.44 to 0.51 g/cm^3) for a 10-year-old loblolly pine trees using X-ray densitometry and also the ranges reported by Jones et al. (2008) ranging from 0.39 to 0.56 g/cm^3 determined for 12-year-old loblolly pine trees. The overall low density of the predicted NIR could be attributed to the spectra that were obtained from the radial section of the core. Several studies have indicated that the spectra collected on the transverse sections were better than models based on spectra acquired from the tangential or radial section, where the difference between transversal and radial measurements was lower in the case of density estimation (Schimleck et al. 2005, Defo et al. 2007, Fujimoto et al. 2007). These differences are related to the direct interference of incident radiation by the cell wall as opposed to the free water in the cell lumen when measured transversely (Tsuchikawa et al. 1996), or they could also be the result of radiation influence on the scattering surface due to roughness differences of the transverse section when compared to the radial section, which is related to particle size differences (Schwanninger et al. 2011).

The effect of wood density on structural wood quality and wood strength properties makes it an important trait for assessing wood quality (Megraw 1985). Several studies have indicated that an increase in absorbance is a characteristic result of increased density (Gindl et al. 2001, Schimleck et al. 2002). Via et al. (2003) showed that an increase in density brought about a 0.27 mean increase in absorbance, which was attributed to baseline shift explained based on having more cell wall material and less lumen diameter, implying that more material is available for absorbance across all wavelengths in the NIR region. The relatively weak dynamic MOE (MOEdy) for both the acoustic estimated and NIR predicted could be attributed to the green density of the outer wood portion of the trunks, and not to a weighted measure of air-dry density at breast height (Isik et al. 2011).

Estimated MOEdy from the acoustic velocity and NIR predicted MOEdy

The MOEdy was estimated from the acoustic velocity and the density of each downed tree. The NIR predicted MOEdy was used to compare with the TOF-estimated MOEdy (Fig. 7). The MOEdy from the offset or opposite face acoustic velocity and the transverse methods were similar and moderately high at estimated predictability of $R^2 \sim 0.70$ at PC 8, compared with the lowest results obtained from the longitudinal method ($R^2 = 0.53$ at PC 7). Similarly, the low MOEdy from the longitudinal measurement may be attributed to the length of travel of the wave (Schimleck et al. 2019). The model for the downed pine dynamic MOE was satisfactory because the prediction capacity was quite good, although the R^2 was not as high as for all the different measuring methods.

The ability of wood to resist loads is characterized by its strength. The strength of the material is usually characterized by the values of its modulus of elasticity (MOE) and its modulus of rupture, MOR. The MOE determines the propagation of the speed of longitudinal waves in the material for a small amplitude of vibration. As wood is considered an elastic material, the MOE is defined as the slope of the stress-strain curve below the linear proportionality limit (Roylance 2001). Acoustic tools have been used to assess standing trees using the TOF acoustic wave, which is measured between the transmitter and receiver probe, in which the sound wave is generated by tapping one end with a light hammer (Wang et al. 2002, Wessels et al. 2011). This

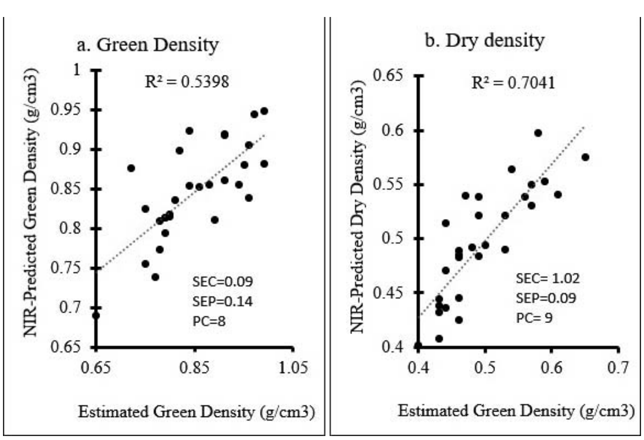

Figure 6.—NIR predicted and estimated density of downed trees.

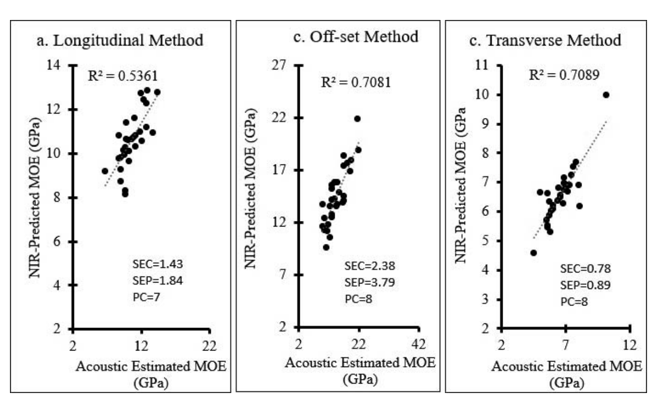

Figure 7.—Relationship between measured and NIR predicted MOE.

can be done even before harvest to enable management, planning, harvesting, and wood processing to be carried out in a way that maximizes extracted value from the resource (Schimleck et al. 2019). It can also be used for downed timber to determine which trees are of the best quality for use in certain applications. The ability to predict the stiffness with these rapid methods could help maximize the values and determine usage, particularly the lumber with dbh around 8 to 11 inches classified as Chip-N-Saw (TMS 2019), the group that is hard to consider in sorting and determination of use and prices due to relative size (bigger than pulp wood but not big enough to be considered saw logs).

Conclusion

This study investigated the applicability of NIR spectroscopy to predict acoustic velocity and estimated MOEdy from acoustic velocity and density. It was demonstrated that NIR spectroscopy from an incremental core sample of downed trees can be successfully used as a high throughput tool to nondestructively screen downed trees for important wood traits such as acoustic velocity, density, and TOF-estimated dynamic MOE. Our results showed that the NIR prediction model for the oven dry density was robust and applicable with a relatively high coefficient of determination when compared to green density. The offset method predicted a relatively high acoustic velocity when compared to the longitudinal and transverse methods.

From the operationality of acoustics and NIR at various points from the stump to the mill point of view, these results are promising, since they demonstrate that acoustics and NIR spectroscopy are efficient tools for the nondestructive measurement/prediction of various wood quality traits. Despite the challenges of determining the properties of interest for fitting the calibration regressions and the relatively time-consuming methods required in taking and collecting cores for the NIR models, when compared to the acoustics, it thus predicts values with detailed profiles which are closer to the acoustics. Therefore, such indirect methods should be considered in the prospects to optimize such technologies in the wood supply chain. The combined features of acoustic and NIR strategy could also be adopted to get a better result. This preliminary study with a smaller sample size is aimed at laying a foundation for further verification to assess the ability of acoustics and NIR in the assessment of damaged trees; more samples are needed in building a more robust model.

Acknowledgments

This research was funded by the USDA Forest Service Down Timber Research Fs-20-Ca-11330170-066-Bv, the McIntire-Stennis (MS) Cooperative Forestry Research Program, and the Hatch Project. The authors declare no conflict of interest. The funders had no role in the design of the study; in the collection, analysis, or interpretation of data; in the writing of the manuscript; or in the decision to publish the results.

Literature Cited

Alves, A., A. Santos, P. Rozenberg, L. E. Pâques, J. P. Charpentier, M. Schwanninger, and J. Rodrigues. 2012. A common near infrared–based partial least squares regression model for the prediction of wood density of Pinus pinaster and Larix× eurolepis. *Wood Sci. Technol*. 46(1–3):157–175.

Baillères, H., F. Davrieux, and F. Ham-Pichavant. 2002. Near infrared analysis as a tool for rapid screening of some major wood characteristics in a eucalyptus breeding program. *Ann. Forest Sci*. 59(5–6):479–490.

Batten, G. D. 1998. An appreciation of the contribution of NIR to agriculture. *J. Near Infrared Spectrosc*. 6(1):105–114.

Beaulieu, J., and P. Dutilleul. 2019. Applications of computed tomography (CT) scanning technology in forest research: A timely update and review. *Can. J. Forest Res*. 49(10):1173–1188.

Belonger, P., S. McKeand, J. Jett, and T. White. 1997. Wood density assessment of diverse families of loblolly pine using X-ray densitometry. *In:* Proceedings of the 24th Southern Forest Tree Improvement Conference, T. White, D. Huber, and G. Powel (Eds.), June 9–12, 1997, Orlando, Florida; US Department of Commerce, Springfield, Virginia. pp. 133–142.

Burns, D. A., and E. W. Ciurczak. 2007. Handbook of Near-Infrared Analysis. CRC Press, Boca Raton, Florida.

Chauhan, S. S., and J. Walker. 2004. Relationships between longitudinal growth strain and some wood properties in Eucalyptus nitens. *Aust. Forestry* 67(4):254–260.

Chauhan, S. S., and J. C. F. Walker. 2006. Variations in acoustic velocity and density with age, and their interrelationships in radiata pine. *Forest Ecol. Manag*. 229(1–3):388–394.

Chen, Z. Q., B. Karlsson, S. O. Lundqvist, M. R. G. Gil, L. Olsson, and H. X. Wu. 2015. Estimating solid wood properties using Pilodyn and acoustic velocity on standing trees of Norway spruce. *Ann. Forest Sci*. 72(4):499–508.

Cieszewski, C. J., M. Strub, F. Antony, P. Bettinger, J. Dahlen, and R. C. Lowe. 2013. Wood quality assessment of tree trunk from the tree branch sample and auxiliary data based on NIR spectroscopy and SilviScan. *Math. Comput. Forestry Natural Res. Sci*. 5(1):86–111.

Cown, D. J. 1978. Comparison of the Pilodyn and torsiometer methods for the rapid assessment of wood density in living trees. *N. Z. J. Forestry Sci*. 8(3):384–391.

Dale, L. M., A. Thewis, C. Boudry, I. Rotar, P. Dardenne, V. Baeten, and J. A. F. Pierna. 2013. Hyperspectral imaging applications in agriculture and agro-food product quality and safety control: A review. *Appl. Spectrosc. Rev*. 48(2):142–159.

Defo, M., A. M. Taylor, and B. Bond. 2007. Determination of moisture content and density of fresh-sawn red oak lumber by near infrared spectroscopy. *Forest Prod. J*. 57(5):68.

Dickson, R. L., B. Joe, P. Harris, S. Holtorf, and C. Wilkinson. 2004. Acoustic segregation of Australian-grown Pinus radiata logs for structural board production. *Aust. Forestry* 67(4):261–266.

Downes, G. M., P. D. Kube, and J. French. 2000. Applications of NIR spectroscopy to forest research. *Appita J*. 53(6):458–464.

Downes, G. M., M. Lausberg, B. M. Potts, D. L. Pilbeam, M. Bird, and B. Bradshaw. 2018. Application of the IML Resistograph to the infield assessment of basic density in plantation eucalypts. *Aust. Forestry* 81(3):177–185.

Downes, G. M., M. Touza, C. Harwood, and M. Wentzel-Vietheer. 2014. NIR detection of non-recoverable collapse in sawn boards of Eucalyptus globulus. *Eur. J. Wood Wood Prod*. 72(5):563–570.

Fomina, N., C. L. McFearin, M. Sermsakdi, J. M. Morachis, and A. Almutairi. 2011. Low power, biologically benign NIR light triggers polymer disassembly. *Macromolecules* 44(21):8590–8597.

Fujimoto, T., H. Kobori, and S. Tsuchikawa. 2012. Prediction of wood density independently of moisture conditions using near infrared spectroscopy. *J. Near Infrared Spectrosc*. 20(3):353–359.

Fujimoto, T., Y. Kurata, K. Matsumoto, and S. Tsuchikawa. 2007. Application of near infrared spectroscopy for estimating wood mechanical properties of small clear and full length lumber specimens. *J. Near Infrared Spectrosc*. 16(6):529–537.

Gäb, M., K. Hoffmann, M. Lobe, R. Metzger, S. Van Ooyen, G. Elbers, and B. Köllner. 2006. NIR-spectroscopic investigation of foliage of ozone-stressed Fagus sylvatica trees. *J. Forest Res*. 11(2):69–75.

Gao, S., X. Wang, M. C. Wiemann, B. K. Brashaw, R. J. Ross, and L. Wang. 2017. A critical analysis of methods for rapid and nondestructive determination of wood density in standing trees. *Ann. Forest Sci*. 74(2):27.

Gendvilas, V., G. M. Downes, M. Neyland, M. Hunt, A. Jacobs, and J.

O'Reilly-Wapstra. 2021. Friction correction when predicting wood basic density using drilling resistance. *Holzforschung* 75(6):508–516.
Gindl, W., A. Teischinger, M. Schwanninger, and B. Hinterstoisser. 2001. The relationship between near-infrared spectra of radial wood surfaces and wood mechanical properties. *J. Near Infrared Spectrosc*. 9(4):255–261.
Hammami, C., F. Rene, and M. Marin. 1999. Process–quality optimization of the vacuum freeze-drying of apple slices by the response surface method. *Int. J. Food Sci. Technol*. 34(2):145–160.
Hoffmeyer, P., and J. G. Pedersen. 1995. Evaluation of density and strength of Norway spruce wood by near-infrared reflectance spectroscopy. *Holz Roh- Werkst*. 53(3):165–170.
Horvath, L., I. Peszlen, P. Peralta, and S. Kelley. 2011. Use of transmittance near-infrared spectroscopy to predict the mechanical properties of 1- and 2-year-old transgenic aspen. *Wood Sci. Technol*. 45(2):303–314.
Hou, Z. Q., Q. Wei, and S. Y. Zhang. 2009. Predicting the density of green logs using the computed tomography technique. *Forest Prod. J*. 59(5):53.
Isik, F., C. R. Mora, and L. R. Schimleck. 2011. Genetic variation in Pinus taeda wood properties predicted using non-destructive techniques. *Ann. Forest Sci*. 68(2):283–293.
Jones, P. D., L. R. Schimleck, R. F. Daniels, A. Clark, and R. C. Purnell. 2008. Comparison of Pinus taeda L. whole-tree wood property calibrations using diffuse reflectance near-infrared spectra obtained using a variety of sampling options. *Wood Sci. Technol*. 42(5):385–400.
Jouan-Rimbaud, D., D.-L. Massart, R. Leardi, and O. E. De Noord. 1995. Genetic algorithms as a tool for wavelength selection in multivariate calibration. *Anal. Chem*. 67(23):4295–4301. https://doi.org/10.1021/ac00119a015
Kelley, S. S., T. G. Rials, L. R. Groom, and C. L. So. 2004. Use of near infrared spectroscopy to predict the mechanical properties of six softwoods. *de Gruyter* 58(3):252–260. https://doi.org/10.1515/HF.2004.039
Kohan, N., B. Via, and S. Taylor. 2013. Prediction of strand feedstock mechanical properties with near infrared spectroscopy. *Bioresources* 7(3):2996–3007.
Launay, J., M. Ivkovich, L. Pâques, C. Bastien, P. Higelin, and P. Rozenberg. 2002. Rapid measurement of trunk MOE on standing trees using RIGIDIMETER. *Ann. Forest Sci*. 59(5–6):465–469.
Launay, J., P. Rozenberg, L. Paques, and J. M. Dewitte. 2000. A new experimental device for rapid measurement of the trunk equivalent modulus of elasticity on standing trees. *Ann. Forest Sci*. 57(4):361–359.
Legg, M., and S. Bradley. 2016. Measurement of stiffness of standing trees and felled logs using acoustics: A review. *J. Acoust. Soc. Am*. 139(2):588–604.
Lindstrom, H., R. Evans, and M. Reale. 2005. Implications of selecting tree clones with high modulus of elasticity. *N. Z. J. For. Sci*. 35(1):50–71.
Lindstrom, H., P. Harris, and R. Nakada. 2002. Methods for measuring stiffness of young trees. *Holz Roh- Werkst*. 60(3):165–174.
Lindstrom, H., P. Harris, C. Sorensson, and R. Evans. 2004. Stiffness and wood variation of 3-year-old Pinus radiata clones. *Wood Sci. Technol*. 38(8):579–597.
Lipp, M. 1996. Comparison of PLS, PCR and MLR for the quantitative determination of foreign oils and fats in butter fats of several European countries by their triglyceride composition. *Z. Lebensm.-Unters. Forsch*. 202(3):193–198. https://doi.org/10.1007/BF01263539
Luypaert, J., D. L. Massart, and Y. Vander Heyden. 2007. Near-infrared spectroscopy applications in pharmaceutical analysis. *Talanta* 72(3):865–883.
Maji, T. K., P. K. Sarkar, P. Kar, B. Liu, P. Lemmens, D. Karmakar, and S. K. Pal. 2019. A combined experimental and computational study on a nanohybrid material for potential application in NIR photocatalysis. *Applied Catalysis A: General* 583:117124.
Martens, H., and M. Martens. 2001. Multivariate Analysis of Quality: An Introduction. John Wiley & Sons, New York.
Megraw, R. A. 1985. Wood quality factors in loblolly pine: The influence of tree age, position in tree, and cultural practice on wood specific gravity, fiber length, and fibril angle. TAPPI Press, Peachtree Corners, Georgia.
Mitsui, K., T. Inagaki, and S. Tsuchikawa. 2008. Monitoring of hydroxyl groups in wood during heat treatment using NIR spectroscopy. *Biomacromolecules* 9(1):286–288.
Mora, C. R., L. R. Schimleck, F. Isik, J. M. Mahon, A. Clark, and R. F. Daniels. 2009. Relationships between acoustic variables and different measures of stiffness in standing Pinus taeda trees. *Can. J. Forest Res*. 39(8):1421–1429.
Musah, M., J. H. Diaz, A. O. Alawode, T. Gallagher, M. S. Peresin, D. Mitchell, M. Smidt, and B. Via. 2022. Field assessment of downed timber strength deterioration rate and wood quality using acoustic technologies. *Forests* 13(5):752.
Nasir, V., S. Nourian, Z. Zhou, S. Rahimi, S. Avramidis, and J. Cool. 2019. Classification and characterization of thermally modified timber using visible and near-infrared spectroscopy and artificial neural networks: A comparative study on the performance of different NDE methods and ANNs. *Wood Sci. Technol*. 53(5):1093–1109.
Palou, A., J. Cruz, M. Blanco, J. Tomàs, J. De Los Ríos, and M. Alcalà. 2012. Determination of drug, excipients and coating distribution in pharmaceutical tablets using NIR-CI. *J. Pharm. Anal*. 2(2):90–97.
Pellerin, R., and R. J. Ross. 2002. Inspection of timber structures using stress wave timing nondestructive evaluation tools. *In:* Nondestructive Evaluation of Wood. R. Pellerin and R. J. Ross (Eds.). Forest Products Society, Madison, Wisconsin.
Prevolnik, M., M. Candek-Potokar, and D. Skorjanc. 2004. Ability of NIR spectroscopy to predict meat chemical composition and quality—A review. *Czech J. Anim. Sci.-UZPI* 49(11)500–510.
Raymond, C. A., and A. C. MacDonald. 1998. Where to shoot your pilodyn: Within tree variation in basic density in plantation Eucalyptus globulus and E. nitens in Tasmania. *New Forests* 15(3):205–221.
Raymond, C. A., and L. R. Schimleck. 2002. Development of near infrared reflectance analysis calibrations for estimating genetic parameters for cellulose content in Eucalyptus globulus. *Can. J. Forest Res*. 32:170–176.
Raymond, C., L. Schimleck, A. Muneri, and A. J. Mitchell. 2001. Genetic parameters and genotype-by-environment interactions for pulp yield predicted using near infrared reflectance analysis and pulp productivity in Eucalyptus globulus. *Forest Genet*. 8:213–224.
Ross, R. J. 2010. Wood handbook: Wood as an engineering material. USDA Forest Service, Forest Products Laboratory, General Technical Report FPL-GTR-190, 509 p.
Roylance, D. 2001. Stress-Strain Curves. Massachusetts Institute of Technology, Cambridge.
Schimleck, L., J. Dahlen, L. A. Apiolaza, G. Downes, G. Emms, R. Evans, J. Moore, L. Pâques, J. Bulcke, and X. Wang. 2019. Non-destructive evaluation techniques and what they tell us about wood property variation. *Forests* 10(9):728.
Schimleck, L. R., and R. Evans. 2002. Estimation of microfibril angle of increment cores by near infrared spectroscopy. *IAWA J*. 23(3):225–234.
Schimleck, L. R., R. Evans, and J. Ilic. 2001. Estimation of Eucalyptus delegatensis wood properties by near infrared spectroscopy. *Can. J. Forest Res*. 31(10):1671–1675.
Schimleck, L. R., R. Evans, P. D. Jones, R. F. Daniels, G. F. Peter, and A. Clark III. 2005. Estimation of microfibril angle and stiffness by near infrared spectroscopy using sample sets having limited wood density variation. *IAWA J*. 26(2):175–187.
Schimleck, L. R., R. Evans, and A. C. Matheson. 2002. Estimation of Pinus radiata D. Don clear wood properties by near-infrared spectroscopy. *J. Wood Sci*. 48(2):132–137. https://doi.org/10.1007/BF00767290
Schimleck, L. R., J. L. M. Matos, R. Trianoski, and J. G. Prata. 2018. Comparison of methods for estimating mechanical properties of wood by NIR spectroscopy. *Journal of Spectrosc*. 2018:4823285. https://doi.org/10.1155/2018/4823285
Schwanninger, M., J. C. Rodrigues, and K. Fackler. 2011. A review of band assignments in near infrared spectra of wood and wood components. *J. Near Infrared Spectrosc*. 19(5):287–308.
Thumm, A., and R. Meder. 2001. Stiffness prediction of radiata pine clearwood test pieces using near infrared spectroscopy. *J. Near Infrared Spectrosc*. 9(2):117–122.

Timber Mart-South (TMS). 2019. TimberMart-South Notes: Products Specifications 2nd Quarter 2019 (p. 5). Timber Mart South. http://timbermart-south.com/pdf/TMSNotes2019.pdf. Accessed January 12, 2022.

Tsuchikawa, S. 2007. A review of recent near infrared research for wood and paper. *Appl. Spectrosc. Rev*. 42(1):43–71.

Tsuchikawa, S., K. Hayashi, and S. Tsutsumi. 1996. Nondestructive measurement of the subsurface structure of biological material having cellular structure by using near-infrared spectroscopy. *Appl. Spectrosc*. 50(9):1117–1124.

Tsuchikawa, S., and H. Kobori. 2015. A review of recent application of near infrared spectroscopy to wood science and technology. *J. Wood Sci*. 61(3):213–220.

Via, B. K., T. F. Shupe, L. H. Groom, M. Stine, and C.-L. So. 2003. Multivariate modelling of density, strength and stiffness from near infrared spectra for mature, juvenile and pith wood of longleaf pine (Pinus palustris). *J. Near Infrared Spectrosc*. 11(5):365–378. https://doi.org/10.1255/jnirs.388

Via, B. K., C. Zhou, G. Acquah, W. Jiang, and L. Eckhardt. 2014. Near infrared spectroscopy calibration for wood chemistry: Which chemometric technique is best for prediction and interpretation? *Sensors* 14(8):13532–13547. https://doi.org/10.3390/s140813532

Viet, D. D., T. Ma, T. Inagaki, N. T. Kim, and S. S.Tsuchikawa, 2021. Near-infrared spectroscopy and hyperspectral imaging can aid in the prediction and mapping of polyploid acacia hybrid wood properties in tree improvement programs. *Holzforschung* 75(12):1067–1080.

Vincent, B., and P. Dardenne. 2021. Application of NIR in agriculture. *In:* Near-Infrared Spectroscopy. Y. Ozaki, C. Huck, S. Tsuchikawa, and S. B. Engelsen (Eds.). Springer, New York. pp. 331–345.

Wang, W., J. J. Qu, X. Hao, Y. Liu, and J. A. Stanturf. 2010. Post-hurricane forest damage assessment using satellite remote sensing. *Agric. Forest Meteorol*. 150(1):122–132.

Wang, X. 2013. Acoustic measurements on trees and logs: A review and analysis. *Wood Sci. Technol*. 47(5):965–975.

Wang, X., P. Carter, R. J. Ross, and B. K. Brashaw. 2007a. Acoustic assessment of wood quality of raw forest materials: A path to increased profitability. *Forest Prod. J*. 57(5):6–14.

Wang, X., R. J. Ross, and P. Carter. 2007b. Acoustic evaluation of wood quality in standing trees. Part I. Acoustic wave behavior. *Wood Fiber Sci*. 39(1):28–38.

Wang, X., R. J. Ross, J. A. Mattson, J. R. Erickson, J. W. Forsman, E. A. Geske, and M. A. Wehr. 2002. Nondestructive evaluation techniques for assessing modulus of elasticity and stiffness of small-diameter logs. *Forest Prod. J*. 52(2):79–85.

Wang, X., R. J. Ross, M. McClellan, R. J. Barbour, J. R. Erickson, J. W. Forsman, and G. D. McGinnis. 2001. Nondestructive evaluation of standing trees with a stress wave method. *Wood Fiber Sci*. 33(4):522–533.

Wessels, C. B., F. S. Malan, and T. Rypstra. 2011. A review of measurement methods used on standing trees for the prediction of some mechanical properties of timber. *Eur. J. Forest Res*. 130(6):881–893.

Wu, S. J., J. M. Xu, G. Y. Li, V. Risto, Z. H. Lu, B. Q. Li, and W. Wang. 2010. Use of the pilodyn for assessing wood properties in standing trees of Eucalyptus clones. *J. Forestry Res*. 21(1):68–72.

Wüst, E., and L. Rudzik. 1996. NIR-Spektroskopische Analytik. *In:* Infrarotspektroskopie. H. Günzler, A. M. Bahadir, R. Borsdorf, K. Danzer, W. Fresenius, R. Galensa, W. Huber, I. Lüderwald, G. Schwedt, and H. Wisser (Eds.). Springer, New York, pp. 217–232.

Zhao, R., X. Zhou, H. Ren, and Y. Wang. 2013. Prediction and correlation analysis of wood air-dry density and elastic modulus for Eucalyptus pellita. *J. Northeast Forestry Univ*. 41(12):68–71.